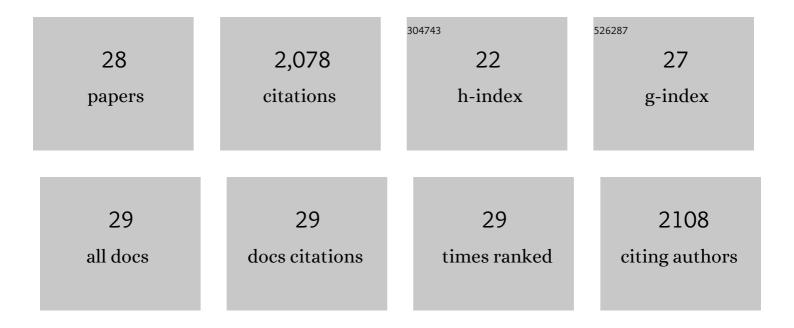
Richard J Walters

List of Publications by Year in descending order

Source: https://exaly.com/author-pdf/3211685/publications.pdf Version: 2024-02-01



#	Article	IF	CITATIONS
1	Interseismic Strain Accumulation Across the Main Recent Fault, SW Iran, From Sentinelâ€1 InSAR Observations. Journal of Geophysical Research: Solid Earth, 2022, 127, .	3.4	8
2	ALADDIn: Autoencoder-LSTM-Based Anomaly Detector of Deformation in InSAR. IEEE Transactions on Geoscience and Remote Sensing, 2022, 60, 1-12.	6.3	5
3	Highâ€Resolution Surface Velocities and Strain for Anatolia From Sentinelâ€1 InSAR and GNSS Data. Geophysical Research Letters, 2020, 47, e2020GL087376.	4.0	108
4	LiCSAR: An Automatic InSAR Tool for Measuring and Monitoring Tectonic and Volcanic Activity. Remote Sensing, 2020, 12, 2430.	4.0	127
5	Partitioned Offâ€Fault Deformation in the 2016 Norcia Earthquake Captured by Differential Terrestrial Laser Scanning. Geophysical Research Letters, 2019, 46, 3199-3205.	4.0	13
6	Constant strain accumulation rate between major earthquakes on the North Anatolian Fault. Nature Communications, 2018, 9, 1392.	12.8	75
7	A Bayesian Method for Incorporating Self‧imilarity Into Earthquake Slip Inversions. Journal of Geophysical Research: Solid Earth, 2018, 123, 6052-6071.	3.4	46
8	Dual control of fault intersections on stop-start rupture in the 2016 Central Italy seismic sequence. Earth and Planetary Science Letters, 2018, 500, 1-14.	4.4	100
9	Constraints from GPS measurements on the dynamics of the zone of convergence between Arabia and Eurasia. Journal of Geophysical Research: Solid Earth, 2017, 122, 1470-1495.	3.4	12
10	The 2008 and 2012 Moosiyan Earthquake Sequences: Rare Insights into the Role of Strike Slip and Thrust Faulting within the Simply Folded Belt (Iran). Bulletin of the Seismological Society of America, 2017, , .	2.3	0
11	Partitioning of oblique convergence coupled to the fault locking behavior of foldâ€andâ€thrust belts: Evidence from the Qilian Shan, northeastern Tibetan Plateau. Tectonics, 2017, 36, 1679-1698.	2.8	89
12	The role of space-based observation in understanding and responding to active tectonics and earthquakes. Nature Communications, 2016, 7, 13844.	12.8	179
13	Interseismic strain accumulation across the central North Anatolian Fault from iteratively unwrapped InSAR measurements. Journal of Geophysical Research: Solid Earth, 2016, 121, 9000-9019.	3.4	86
14	Geodetic observations of postseismic creep in the decade after the 1999 Izmit earthquake, Turkey: Implications for a shallow slip deficit. Journal of Geophysical Research: Solid Earth, 2016, 121, 2980-3001.	3.4	40
15	Normal faulting in the Simav graben of western Turkey reassessed with calibrated earthquake relocations. Journal of Geophysical Research: Solid Earth, 2016, 121, 4553-4574.	3.4	21
16	Spatial variations in fault friction related to lithology from rupture and afterslip of the 2014 South Napa, California, earthquake. Geophysical Research Letters, 2016, 43, 6808-6816.	4.0	62
17	The 2013 <i>M</i> _{<i>w</i>} 6.2 Khakiâ€Shonbe (Iran) Earthquake: Insights into seismic and aseismic shortening of the Zagros sedimentary cover. Earth and Space Science, 2015, 2, 435-471.	2.6	38
18	Statistical comparison of InSAR tropospheric correction techniques. Remote Sensing of Environment, 2015, 170, 40-47.	11.0	278

RICHARD J WALTERS

#	Article	IF	CITATIONS
19	Systematic assessment of atmospheric uncertainties for InSAR data at volcanic arcs using large-scale atmospheric models: Application to the Cascade volcanoes, United States. Remote Sensing of Environment, 2015, 170, 102-114.	11.0	72
20	Constraining crustal velocity fields with InSAR for Eastern Turkey: Limits to the blockâ€like behavior of Eastern Anatolia. Journal of Geophysical Research: Solid Earth, 2014, 119, 5215-5234.	3.4	67
21	Coseismic and post-seismic slip of the 2009 L'Aquila (central Italy) MW 6.3 earthquake and implications for seismic potential along the Campotosto fault from joint inversion of high-precision levelling, InSAR and GPS data. Tectonophysics, 2014, 622, 168-185.	2.2	49
22	The 2010–2011 South Rigan (Baluchestan) earthquake sequence and its implications for distributed deformation and earthquake hazard in southeast Iran. Geophysical Journal International, 2013, 193, 349-374.	2.4	57
23	Rapid strain accumulation on the Ashkabad fault (Turkmenistan) from atmosphere orrected InSAR. Journal of Geophysical Research: Solid Earth, 2013, 118, 3674-3690.	3.4	57
24	Interseismic strain accumulation across the North Anatolian Fault from Envisat InSAR measurements. Geophysical Research Letters, 2011, 38, n/a-n/a.	4.0	52
25	The 2010 <i>M</i> _{<i>W</i>} 6.8 Yushu (Qinghai, China) earthquake: Constraints provided by InSAR and body wave seismology. Journal of Geophysical Research, 2011, 116, .	3.3	84
26	Shallow subsurface structure of the 2009 April 6 Mw 6.3 L'Aquila earthquake surface rupture at Paganica, investigated with ground-penetrating radar. Geophysical Journal International, 2010, 183, 774-790.	2.4	32
27	Extension on the Tibetan plateau: recent normal faulting measured by InSAR and body wave seismology. Geophysical Journal International, 2010, 183, 503-535.	2.4	146
28	The 2009 L'Aquila earthquake (central Italy): A source mechanism and implications for seismic hazard. Geophysical Research Letters, 2009, 36, .	4.0	174